

A HaloTag-Based Small Molecule Microarray Screening Methodology with Increased Sensitivity and Multiplex Capabilities

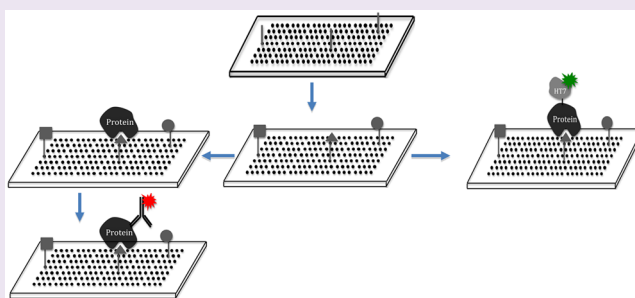
Devin J. Noblin,[†] Charlotte M. Page,[†] Hyun Seop Tae,[†] Peter C. Gareiss,[‡] John S. Schneckloth,[‡] and Craig M. Crews^{*,†,§,||}

Departments of [†]Molecular Cellular and Developmental Biology, [§]Chemistry, and ^{||}Pharmacology, Yale University, 219 Prospect Street, New Haven, Connecticut 06511, United States

[‡]Yale Center for Molecular Discovery, 100 West Campus Drive, Orange, Connecticut 06477, United States

S Supporting Information

ABSTRACT: Small Molecule Microarrays (SMMs) represent a general platform for screening small molecule–protein interactions independent of functional inhibition of target proteins. In an effort to increase the scope and utility of SMMs, we have modified the SMM screening methodology to increase assay sensitivity and facilitate multiplex screening. Fusing target proteins to the HaloTag protein allows us to covalently prelabel fusion proteins with fluorophores, leading to increased assay sensitivity and an ability to conduct multiplex screens. We use the interaction between FKBP12 and two ligands, rapamycin and ARIAD's "bump" ligand, to show that the HaloTag-based SMM screening methodology significantly increases assay sensitivity. Additionally, using wild type FKBP12 and the FKBP12 F36V mutant, we show that prelabeling various protein isoforms with different fluorophores allows us to conduct multiplex screens and identify ligands to a specific isoform. Finally, we show this multiplex screening technique is capable of identifying ligands selective for a specific PTP1B isoform using a 20,000 compound screening deck.



As little as 20% of the human proteome can be targeted by traditional small molecule inhibitors, leaving a vast “undruggable proteome”.^{1,2} Several academic laboratories have developed methods to downregulate target protein levels in cells using small molecules, obviating the need for enzymatic inhibition and thereby allowing access to much of this undruggable proteome. For example, PROteolysis TARgeting Chimeric moleculeS (PROTACS)^{3–6} are heterobifunctional molecules that comprise a ligand for the target protein, a linker moiety, and a ligand for an E3 ubiquitin ligase. Upon addition to cells, PROTACS induce the colocalization of the target protein and E3 ligase, resulting in ubiquitination and subsequent proteasome-mediated degradation of the target protein. In another example, taking ligands to a target protein and coupling them to a hydrophobic group can yield a hydrophobic tag^{7,8} that induces proteasome-mediated degradation of the target protein upon binding. These methods hold particular appeal because they do not require a ligand that inhibits functional activity of the target protein. Any ligand that binds to a target protein could, in principle, be incorporated into a PROTAC or hydrophobic tag to degrade the target protein. Therefore, strategies aimed at targeting currently undruggable proteins would benefit greatly from a general method to identify ligands irrespective of functional inhibition.

Small Molecule Microarrays (SMMs)^{9,10} provide a rapid assay format suitable for small molecule screening and do not require inhibition of protein activity as a readout of binding.

Bradner *et al.*¹¹ provide a detailed SMM protocol upon which we have based our past SMM screening attempts (schematic found in Figure 1). Briefly, according to the Bradner protocol, Gamma Amino Propyl Silane (GAPS II) slides are functionalized with an isocyanatohexane linker that reacts with small molecules containing primary alcohols and amines. Next, approximately 10,000 small molecules are robotically printed onto each slide, and covalent attachment is catalyzed by exposure to pyridine vapor. Then the slides are quenched with ethylene glycol and stored for use. To screen for ligands, Bradner and colleagues incubated microarray slides with their target proteins and subsequently detected the proteins with fluorophore-conjugated antibodies. As a result, putative ligands appeared as fluorescent spots on the array slide. Several orthogonal techniques, such as differential scanning fluorimetry,¹² can provide secondary validation of identified ligands.

The majority of published works have focused on improving SMM sensitivity through various methods of surface modification. Examples include immobilization of thiols on maleimide-derivatized slides,⁹ silyl chloride-derivatized slides,¹³ diazobenzylidene-mediated immobilization,¹⁴ isocyanate-derivatized slides,¹⁵ and 3D hydrogel SMMs.¹⁶ Using these slide surfaces, several groups have reported using SMMs to identify

Received: August 24, 2012

Accepted: September 26, 2012

Published: September 26, 2012

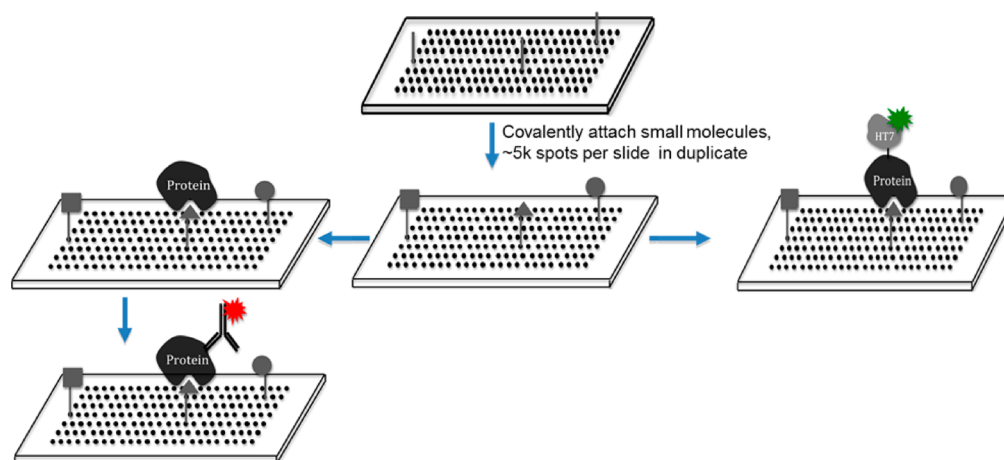


Figure 1. Schematic of SMM screening using antibody-based (left) or HaloTag-based (right) methodologies. Four arrays were prepared, each containing ~5,000 compounds printed in duplicate at a concentration of 10 mM, as described by Bradner *et al.*¹¹ One array included 3-fold serial dilutions of rapamycin and the ARIAD bump ligand. In both screening methodologies, slides were initially blocked with 1 μ M GST-HaloTag and then washed. At this point, the two techniques diverge: In the antibody-based technique, slides were incubated for 1 h with 500 nM protein, washed, and then incubated with an AlexaFluor647-conjugated anti-(His)₅ antibody for 1 h. In the HaloTag-based technique, slides were incubated for 1 h with 50 nM fluorophore-labeled HaloTag fusion protein. In both techniques, after incubation with the protein of interest, slides were washed, spun dry, and then scanned with a GenePix 4000a Microarray Scanner.

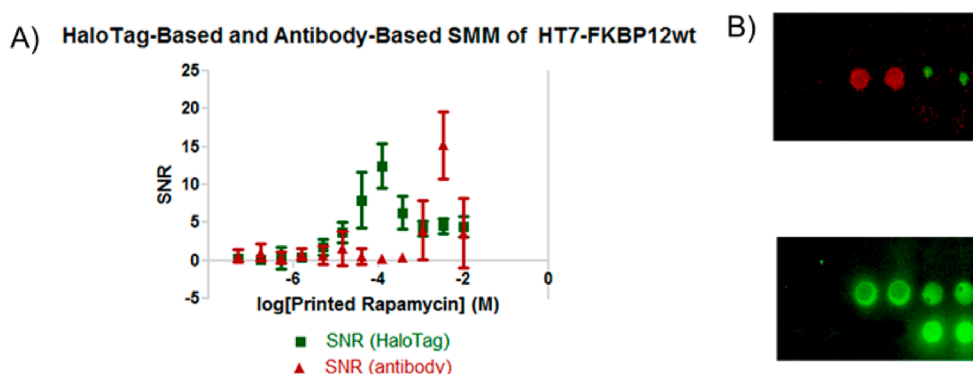


Figure 2. Direct comparison of antibody-based and HaloTag-based SMM methodologies using (His)₆-HaloTag-FKBP12 on identically printed SMM slides. Rapamycin was printed in 3-fold serial dilution from a top concentration of 10 mM. (A) The average and SEM of SNR values for each concentration of rapamycin spots in each technique, antibody-based (red) and HaloTag-based (green). The HaloTag-based technique detects the FKBP12-rapamycin interaction at a lower concentration of printed compound than the antibody-based technique does. Additionally, optimal signal was obtained by incubating slides with 50 nM protein in the HaloTag-based technique, which is 10-fold lower than the 500 nM protein required to achieve significant signal in the antibody-based technique. Signal-to-noise (SNR) values exhibit an abnormal decrease at extremely high concentrations of printed compound due to signals bleeding beyond the predefined spots in the genepix array file (confirmed by examining raw fluorescence values), thereby increasing the calculated background values. We did not adjust screening conditions based on this abnormality because spot size was determined on the basis of optimal signal for lower-affinity interactions, which do not exhibit this abnormality. Additionally, the rapamycin-FKBP12 interaction would be detected as a hit using the HaloTag-based technique despite this abnormality. (B) Representative images of 10 mM rapamycin spots after either antibody-based (top) or HaloTag-based (bottom) SMM assay. The two middle spots are the compound of interest printed in duplicate. Antibody-based (top) and HaloTag-based (bottom) spots are both bright and highly visible.

ligands to target proteins, including proteins such as transcription factors that would normally be considered undruggable.^{10,17}

Despite the great potential of SMMs, the success rate in our experience has been low. Whereas the work described above attempted to improve SMM technology by focusing on surface modification, herein we focused instead on the methods used to detect probed proteins. We hypothesized that the secondary antibody incubation step and subsequent washes often required in traditional SMM screening techniques may allow protein to dissociate from its immobilized ligand, thereby reducing assay sensitivity. This effect would be particularly detrimental when screening a small compound deck that may only contain modest affinity ligands to the target protein. We reasoned that

covalently labeling the recombinant protein with a fluorophore before screening would allow us to eliminate the antibody incubation step and thus potentially increase assay sensitivity.

Covalent attachment of organic dyes holds advantage over creating GFP fusion proteins since GFP has a relatively low extinction coefficient compared to many commercially available fluorophores.¹⁸ Although several groups report direct labeling of proteins with fluorophores in SMM assays,^{9,16} their applications have been limited in scope. Additionally, direct labeling of the target protein surface can disrupt ligand-binding pockets containing functional groups such as sulfhydryl groups. Instead, we turned to the HaloTag system, developed by Promega, whereby fusing the 33 kDa HaloTag protein to a protein of interest allows covalent labeling with chloroalkane-

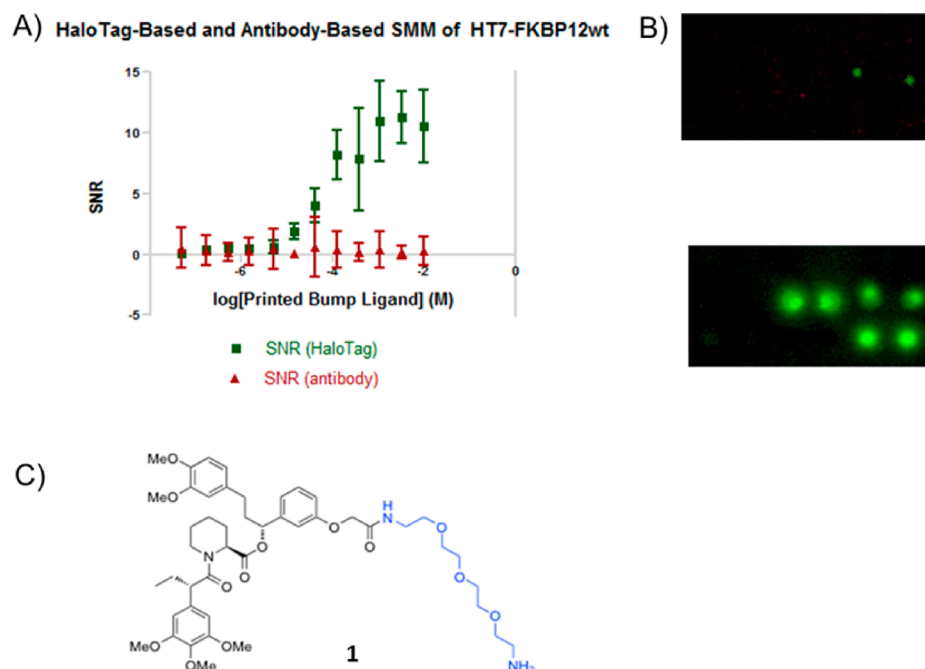


Figure 3. Direct comparison of antibody-based and HaloTag-based SMM methodologies using (His)₆-HaloTag-FKBP12 on identically printed SMM slides. The derivatized ARIAD bump ligand, compound 1, was printed in 3-fold serial dilution from a top concentration of 10 mM. (A) The average and SEM of SNR values for each concentration of ARIAD bump ligand spots in each technique, antibody-based (red) and HaloTag-based (green). The HaloTag-based technique detects the FKBP12-ARIAD bump ligand interaction, whereas the antibody-based technique does not. Note that this lower-affinity FKBP12-ARIAD bump ligand interaction does not display the abnormal decrease in SNR at high concentrations of printed compound as observed with rapamycin. (B) Representative images of 10 mM ARIAD bump ligand spots after either antibody-based (top) or HaloTag-based (bottom) SMM assay. The two middle spots are compound of interest printed in duplicate. The antibody-based technique (top) has no visible spots, whereas the HaloTag-based technique (bottom) has two bright spots. (C) Structure of the derivatized ARIAD bump ligand printed on SMM slides. Slide-reactive linker is colored blue.

derivatized fluorophores.¹⁹ Prelabeling HaloTag-fused proteins with fluorophores should increase assay sensitivity, permitting the identification of lower-affinity small molecule–protein interactions and facilitating multiplex SMM assays. In this paper, we validate our system using the interaction between the FK-506 binding protein (FKBP12)²⁰ and two ligands, rapamycin²¹ and a “bump” ligand developed by ARIAD Pharmaceuticals.²² We then demonstrate the utility of our assay by screening a 20,000 compound library and identifying several ligands selective for protein tyrosine phosphatase 1B (PTP1B) trapped in the first transition state of phosphatase catalysis.

RESULTS AND DISCUSSION

Directly Comparing Antibody-Based and HaloTag-Based SMM. To validate our system, we turned to the interaction between the FK-506 binding protein (FKBP12)²⁰ and two ligands, rapamycin²¹ and a bump ligand developed by ARIAD Pharmaceuticals.²² Rapamycin binds to wild type FKBP12 with a reported K_d of 0.02 nM,²³ whereas the ARIAD bump ligand binds to wild type FKBP12 with a reported K_d of 67 nM.²² ARIAD's bump ligand exhibits nearly 1000-fold selectivity for the F36V mutant (reported K_d of 0.094 nM for the mutant FKBP12 F36V *versus* reported K_d of 67 nM for wild type FKBP12),²² whereas rapamycin exhibits similar affinity for both proteins. The (His)₆-HaloTag-FKBP12 wild type protein (FKBP12wt) allowed us to compare directly the antibody-based and HaloTag-based SMM protocols. It is important to stress that the same stock of protein was used in both protocols,

as the protein contains both the histidine tag required for antibody detection and HaloTag for covalent prelabeling.

Figure 2 evaluates the interaction of FKBP12wt with spots on the microarray containing rapamycin printed at various concentrations. An increase in signal-to-noise ratio (SNR) can be detected at a lower concentration of printed rapamycin in the HaloTag-based technique, compared to the antibody-based SMM (Figure 2A). Optimal screening conditions using the HaloTag-based technique enabled usage of 10-fold less protein than the antibody-based technique (50 *versus* 500 nM, respectively), further supporting the hypothesis that a significant amount of protein dissociates from the slide during the antibody incubation and associated wash steps. It was surprising to note that SNR values initially increased with increasing compound concentrations and then, after reaching a maximal value, decreased with higher compound concentrations. By visually inspecting the raw fluorescence intensity of each spot, we have confirmed this abnormality, which is a result of high signal intensity bleeding into the surrounding area background, thereby decreasing the apparent ratio of signal-to-noise. Although the assay protocol could be modified to eliminate this abnormality, this protein–ligand interaction would still have been identified in the current screening format. Instead, we chose to optimize the assay to identify lower-affinity interactions, represented by the FKBP12wt interaction with the ARIAD bump ligand, discussed below.

Since the HaloTag-based SMM identified the FKBP12–rapamycin interaction at a lower concentration of printed compound, we reasoned that the HaloTag-based SMM detection strategy may also be able to identify lower affinity

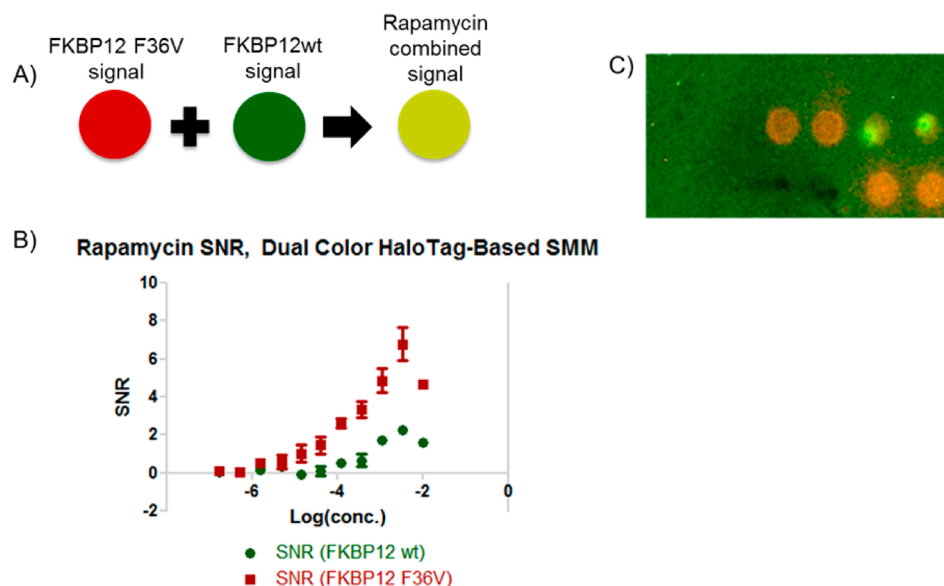


Figure 4. HaloTag-based SMM can detect the interaction of rapamycin with both wild type FKBP12 (FKBP12wt, labeled green) and the mutant FKBP12 F36V (FKBP12 F36V, labeled red) incubated on the same slide. (A) Schematic: Since rapamycin binds to both wild type and mutant FKBP12 with similar affinities, the spots should exhibit both green and red fluorescence. (B) Average and SEM of each concentration of rapamycin in both the red and green channels. (C) Representative images of 10 mM rapamycin spots after multiplex HaloTag-based SMM assay. The two middle spots are the compound of interest printed in duplicate. Spots contain signal in both red and green channels.

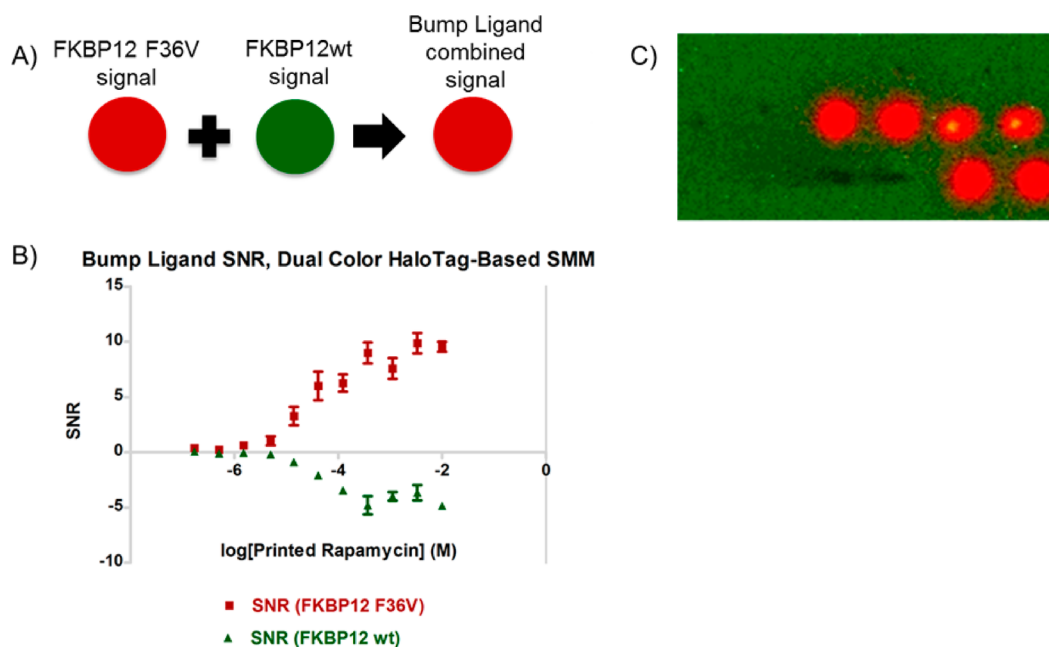


Figure 5. HaloTag-based SMM detection methodology can identify the specific interaction of ARIAD bump ligand with FKBP12 F36V (labeled red) when co-incubated with FKBP12wt (labeled green) on the same slide. (A) Schematic: Since the ARIAD bump ligand binds to mutant FKBP12 with 1000-fold greater affinity than FKBP12wt, the spots should exhibit strictly red fluorescence. (B) Average and SEM of each concentration of ARIAD bump ligand in both the red and green channels. Note that the binding of FKBP12 F36V occludes the weaker binding FKBP12wt even at background levels and thus results in a negative SNR in the green channel. (C) Representative images of 10 mM ARIAD bump ligand spots after multiplex HaloTag-based SMM assay. The two middle spots are the compound of interest printed in duplicate. Spots contain positive signal in the red channel and below-background signal in the green channel.

ligands printed at a high compound concentration. To test this hypothesis, we synthesized a derivatized version of the ARIAD bump ligand (1, structure in Figure 3C, synthesis and characterization in Supporting Information), reported to have a similarly tight interaction with the FKBP12 F36V mutant but a 1000-fold weaker interaction with wild type FKBP12, as described earlier. This compound was printed onto array slides

in the same serial dilution pattern as described above for rapamycin. The HaloTag-based SMM was able to detect the 1000-fold weaker interaction of the ARIAD bump ligand with wild type FKBP12, but the antibody-based SMM could not detect an interaction at any concentration of printed compound (Figure 3A). This result supports our hypothesis that the antibody incubation step in the antibody-based SMM detection

technique may be particularly inadequate when attempting to identify weaker small molecule–protein interactions.

Multiplex Screening To Identify Isoform-Specific Ligands. We hypothesized that the HaloTag-based SMM may also provide a better system to screen multiple proteins on the same slide, each protein labeled with a different fluorophore. Such a screening format could reduce the costs of screening multiple target proteins with the same library and could also facilitate interesting screens for ligands specific to a particular protein isoform of interest. Thus, we treated a single slide, containing both rapamycin and ARIAD bump ligand spots, with HaloTag-fused FKBP12 wild type (FKBP12wt) and F36V mutant (FKBP12 F36V) proteins. We performed a dual color SMM screen using FKBP12wt labeled with halo-TMR (green) and FKBP12 F36V labeled with halo-Dye633 (red). Rapamycin, which has a similar affinity for both proteins, showed a positive signal in both red and green channels with a similar dose response (Figure 4). The ARIAD bump ligand, which has a nearly 1000-fold greater affinity for the mutant FKBP12 F36V protein, had a strong signal in the red channel but a negative SNR in the green channel (Figure 5).

Comparing rapamycin spots with ARIAD bump ligand spots led us to speculate about several general properties of a multiplex SMM screen. First, rapamycin had lower maximal SNR values in the FKBP12wt wavelength in the dual color screen, presented in Figure 4, than it did in the single color screen, presented in Figure 2. Therefore, screening multiple proteins on the same slide may reduce the SMM's ability to identify nonspecific ligands, as the multiple proteins may compete with each other for available binding sites. Second, the signal from FKBP12wt (green fluorescence in our experiment) had a negative SNR in the bump ligand spots on the dual color screen. We suspect this effect occurs because FKBP12 F36V has a higher affinity for the immobilized bump ligand, whereby FKBP12 F36V is bound in sufficient quantity to occlude simultaneous FKBP12wt binding. By comparing SNR values in the two wavelengths used, the dual color SMM may therefore have an increased capacity to identify protein-specific ligands compared to a single color SMM.

On the basis of the above observations, we propose several considerations for designing an appropriate SMM screen. Screening multiple proteins on a single slide will increase the ability to detect ligands specific to a particular protein isoform, since the positive SNR signal in one fluorescence channel will be coupled with a negative SNR signal in the other channel. Additionally, multiplexing will reduce the number of screens required to identify isoform-specific ligands. Co-screening protein isoforms may, however, reduce the ability of the SMM to identify ligands that are nonspecific binders, as the target proteins will compete for binding sites and therefore split the resulting SNR signal. An area of potential improvement in our assay is the quality of compound printing on the array, as variability from slide to slide exists in both spot morphology and location. Inconsistent spot morphology could be the result of either asymmetric drying effects or variable surface chemistry. Future efforts to solve this problem should focus on varying arraying pins, surface chemistry, solution concentration, or drying conditions.

Screening for Ligands Specific to PTP1B Transition State Analogues. To demonstrate the utility of this multiplex HaloTag-based SMM technique, we chose to screen for ligands to the protein tyrosine phosphatase 1B (PTP1B), which is an attractive therapeutic target that has so far proven challenging

for drug development efforts. PTP1B is a protein tyrosine phosphatase responsible for downregulating several biological pathways, including the insulin pathway *via* dephosphorylation of the insulin receptor²⁴ and the leptin pathway *via* dephosphorylation of the leptin receptor.²⁵ PTP1B knockout mice under high-fat diets exhibit obesity resistance,²⁶ and antisense oligonucleotide treatment restores insulin sensitivity in diabetic mice.²⁷ Despite the widespread desire to target PTP1B, no competitive and specific small molecule inhibitors have yet entered the clinic. Two major hurdles, namely, specificity and cell permeability, have stymied the development of small molecule PTP1B inhibitors. First, PTP1B shares 74% sequence identity with the related protein tyrosine phosphatase TCPTP in the catalytic region, and TCPTP knockout results in B- and T-cell abnormalities.²⁸ Second, many small molecules that inhibit the charged active site are hydrophilic and therefore cell impermeable.²⁹ Thus, PTP1B represents a so-far “undruggable” protein for which nonactive site ligands would be useful. Crystallographic studies by Brandão *et al.*³⁰ recently suggested that trapping PTP1B in a transition state of its catalysis may expose new binding pockets for nonactive site ligands. Such ligands would serve as scaffolds for future therapeutically useful compounds and would demonstrate the utility of a multiplex HaloTag-based SMM screening strategy. To screen for ligands to the PTP1B transition state analogue, we prebound HaloTag-PTP1B with sodium orthovanadate complexed with a peptide containing the EGFR-derived PTP1B substrate sequence, Asp-Ala-Asp-Glu-Tyr-Leu, as described.³⁰ We then labeled this transition state analogue with halo-Dye633 (TSA PTP1B, red) and labeled apo HaloTag-PTP1B with halo-TMR (apo PTP1B, green). We co-screened these apo PTP1B and TSA PTP1B proteins and identified three hits specific to TSA PTP1B (Table 1).

Using a thermal shift assay, we were able to validate solution phase binding to PTP1B without a HaloTag fusion for one of the compounds, **5** (Figure 6). The specificity of **5** toward TSA PTP1B was maintained in solution phase, as an increase in melting temperature was seen at a lower concentration of **5** for the transition state analogue than for the apo protein. Of note, **5** did not inhibit PTP1B phosphatase activity as measured *via* hydrolysis of *p*-nitrophenyl phosphate (Figure 6), suggesting **5** binds to but does not inhibit the catalytic function of PTP1B.

We next assayed a number of commercially available compounds that shared structural features with **5** in the hopes of finding a more potent ligand or an allosteric inhibitor. Table 2 lists the compounds evaluated against TSA PTP1B and apo PTP1B in a thermal shift assay and a qualitative measure of their thermal shifts as compared to **5**. No compounds exhibited a greater degree of thermal shift than **5**. None of the compounds inhibited PTP1B phosphatase activity. We did notice that several TSA PTP1B ligands share a hydroxyquinoline group with **5**. Hydroxyquinoline is known to interact with vanadate,³¹ so we suspect the observed specificity toward TSA PTP1B is actually a specificity toward orthovanadate-bound PTP1B. Although we see no physiological use for such ligands, our data demonstrate that the HaloTag-based SMM allowed us to identify ligands specific to a particular isoform of PTP1B by screening a 20,000 compound library.

Conclusions. Low reagent requirements and rapid assay time make SMM screening particularly amenable to academic discovery programs. However, in order to cater to the specific needs of various academic groups, SMMs must be capable of detecting weaker small molecule–protein interactions in order

Table 1. Hits from a Screen for Ligands Specific to the First Transition State Analogue of PTP1B (TSA PTP1B)^a

Compound ID	Structure	Apo PTP1B Z-score	TSA PTP1B Z-score
2		2.77	0.58
3		4.44	-2.13
4		-1.83	11.47
5		-4.05	6.43
6		-5.28	6.76

^aPTP1B, pre-bound with an orthovanadate-DADEYL peptide complex (TSA PTP1B), was labeled with a red fluorophore; apo PTP1B was labeled with a green fluorophore. Both proteins were co-incubated on SMM slides comprising approximately 20,000 different small molecules, each printed in duplicate.

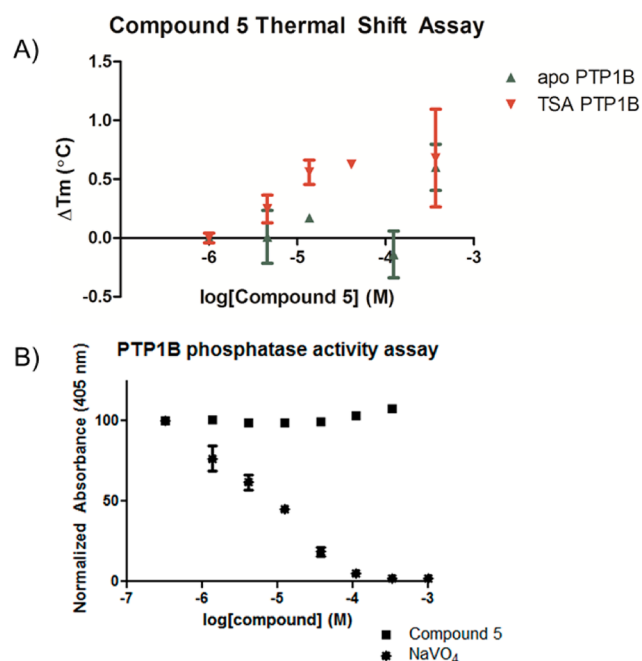


Figure 6. Compound 5 was validated as a TSA PTP1B-specific ligand in *in vitro* assays. (A) Using a thermal shift assay, an increase in TSA PTP1B melting temperature was observed at a lower concentration of 5 than for apo PTP1B. (B) Using a pNPP assay, no inhibition of PTP1B phosphatase activity was detected (sodium orthovanadate, a known tyrosine phosphatase inhibitor, was used as a positive control).

Table 2. Qualitative Representation of Results from Thermal Shift Assays Used To Test Several Commercially Available Compounds Sharing Common Structural Features with 5^a

Compound ID	Structure	Thermal shift with apo PTP1B	Thermal shift with TSA PTP1B
5		+	++
7		-	-
8		+	+
9		-	-
10		+	++
11		+	+
12		+	+
13		-	-
14		++	++
15		+	+
16		+	+
17		-	-
18		-	-
19		++	-
20		-	-
21		-	-

^aAlthough no compounds exhibited increased TSA PTP1B binding compared to that of 5, several TSA PTP1B ligands shared a hydroxyquinoline group with 5.

to be useful. We hypothesized that covalent prelabeling of protein with fluorophore, using the HaloTag system, should allow one to avoid the secondary antibody incubation period, during which protein can dissociate from ligands on the array, thereby increasing assay sensitivity.

Indeed, the HaloTag-based technique was more sensitive in identifying both the high-affinity rapamycin-FKBP12 interaction and the 1000-fold weaker ARIAD bump ligand-FKBP12

interaction. Additionally, we showed that the HaloTag-based technique allows for multiplex screening, labeling various protein isoforms each with a different fluorophore and assaying them simultaneously on a single array slide, to identify isoform-specific ligands. We validated this approach using the ARIAD bump ligand, which has a 1000-fold selectivity toward the F36V mutant FKBP12 over wild type FKBP12. Applying the approach in screening a 20,000 compound library, we identified ligands selective to PTP1B bound with an orthovanadate–substrate peptide complex.

In conclusion, we have developed a method of SMM screening that is more amenable to lead discovery efforts. Prelabeling HaloTag-fused recombinant proteins increases sensitivity for weak protein–small molecule interactions, thereby making the SMM better suited for the compound libraries typically found in academic groups. This HaloTag-based approach requires 10-fold lower protein concentrations and can be modified to screen multiple proteins on a single slide, further reducing the reagent costs and assay time using SMM technology. These improvements, coupled with the inherent advantages of the SMM technology, enhance the utility of SMM screening in lead discovery programs.

METHODS

Generating Recombinant HaloTag-Fused Protein. To generate fusion protein expression vectors, first the coding sequence for HaloTag lacking a stop codon was subcloned into the pET-28a(+) vector (Invitrogen) downstream of the (His)₆ tag using the NheI and BamHI restriction sites. Subsequently, each fusion protein was subcloned downstream of HaloTag using the SalI and NotI restriction sites. Primers for each protein are as follows:

HaloTag forward: GGTGCTAGCGCAGAAATCGG-TACTGGCTT

HaloTag reverse: CCGGATCCTTCCATGGCGATCGCGTT

PTP1B forward: GGTGTCGACATGGAGATGGAAAAG-GAGTTCCG

PTP1B reverse: GGTGCGGCCGCTCAATTGTGTGGCTC-CAGGATTC

FKBP12 forward: GGTGTCGACATGGGAGTGCAGGTG-GAA

FKBP12 reverse: GGTGCGGCCGCTCATTCCAGTTTGA-GAAGCTCCA

The resulting plasmids were then introduced into BL21 (DE3) PLYS chemically competent *E. coli* (Invitrogen). Two liters of these bacteria were induced in exponential phase using 1 mM IPTG at RT for 16 h. The bacteria were then resuspended in the equilibration buffer used with the HisPur Cobalt Purification Kit (Thermo Scientific), to which 0.1% NP40 and Complete Protease Inhibitor Cocktail Tablets (Roche) were added. The bacteria were lysed using a Branson Sonifier 450, and cellular debris was removed by centrifugation at 10,000g for 10 min. The recombinant protein was purified using the HisPur Cobalt Purification Kit (Thermo Scientific) and then dialyzed 1:100 against DPBS (Gibco) two times. Dialyzed proteins were assayed for purity using a Coomassie stain, and protein levels were quantified using the Bio-Rad Protein Assay. Protein activity was validated by incubating 1 μ M purified fusion protein with 2 μ M halo-TMR ligand (Promega), incubating the reaction for 10 min, running the reaction on a 10% acrylamide gel, and visualizing TMR fluorescence. PTP1B activity was validated using a pNPP phosphatase assay, described below.

Preparation of Proteins for HaloTag SMM Technique. For the SMMs with fluorophore-labeled FKBP12, proteins were labeled by incubating the desired version of HaloTag-FKBP12 with fluorophore in a 2:1 ratio for 10 min at RT. The wild type FKBP12 fusion protein, (His)₆-HaloTag-FKBP12 (FKBP12wt), was labeled with halo-TMR (Promega), while the F36V mutant-containing (His)₆-HaloTag-

FKBP12 F36V (FKBP12 F36V) was labeled with halo-Dye633 (Promega). The labeled proteins were diluted in PBST (PBS from GIBCO spiked with 0.1% TBST), and a PD-10 buffer exchange column (GE Healthcare) was utilized to remove excess fluorophore. For the SMM with TMR-labeled FKBP12wt alone, the SMM was incubated with 50 nM protein. For the dual color SMM with both TMR-labeled FKBP12wt and Cy5-labeled FKBP12 F36V, 25 nM concentration of each protein was used.

For the PTP1B dual color SMM, apo PTP1B was prepared in the same manner as FKBP12 described above. Labeled PTP1B trapped in the first transition state (TSA PTP1B) was prepared by incubating 1 μ L of 5 mM NaVO₄ with 1 μ L of 5 mM NH₂-DADEYL-COOH peptide (in 10 mM Tris pH 8.5) for 1 h at RT, then adding 50 μ L of 15 μ M HaloTag-PTP1B and 1 μ L of 5 mM halo-Dye633, and incubating for another 10 min at RT. This reaction mixture was dialyzed 1:4000 in PBS with 3 mM DTT for 30 min. The two labeled forms of HaloTag-PTP1B were diluted with PBST, passed through separate buffer exchange columns, and then combined to probe the SMM. The incubation on SMM slides consisted of 10 nM TMR-labeled apo PTP1B and 10 nM Dye633-labeled TSA PTP1B.

Small-Molecule Microarray (SMM) Protocol. A schematic for the screening process for SMM slides, including both the antibody and HaloTag techniques, is provided in Figure 1. Slides were printed at the Yale Center for Molecular Discovery following the protocol from Bradner *et al.*¹¹ Four arrays were printed, each containing approximately 5,000 different small molecules in duplicate, for a library size of roughly 20,000 molecules selected from the Yale Center for Molecular Discovery's small molecule library. One of the arrays included the ARIAD bump ligand and rapamycin at a 3-fold serial dilution, with 50 replicate spots for the top concentration of 10 mM and 8 replicate spots for all other concentrations.

First, slides were blocked with 1 μ M GST-HaloTag in PBST for 1 h, followed by three 5-min washes with PBST. The protocols for the antibody- and HaloTag-detection techniques diverged at the next step. In the antibody-detection technique, the blocked slide was incubated for 1 h with 500 nM protein in PBST, followed by three 5 min washes with PBST, and then incubated with an AlexaFluor647-conjugated anti-(His)₅ antibody, 1:2000 in PBST, for 1 h. In the HaloTag technique, the blocked slide was incubated for 1 h with 50 nM fluorophore-labeled HaloTag fusion protein in PBST. In both techniques, after incubation with the protein of interest, the slides were washed three times with PBST, two times with PBS, and finally once with deionized water, for 5 min each. The washed slides were placed in 50 mL Falcon tubes, with Kimwipes at the bottom to collect liquid and spun dry for 2 min at 3400g in a centrifuge (IEC Centra CL3R). The dried slides were scanned with a GenePix 4000a Microarray Scanner.

Analysis of SMM Data. For each slide screened with the GenePix scanner, the scanned image was aligned with the appropriate GenePix Array List (GAL) file using GenePix Pro 6.1 software, and the resulting GPR file was analyzed using JMP 9.0 (SAS). For the PTP1B screen, hit analysis was performed using the protocol previously developed at the Yale Center for Molecular Discovery. First, signal-to-noise ratio (SNR) values for replicate spots were averaged. The SMM slides used in this experiment included two spots for each screened compound and numerous spots for the control, DMSO. The mean (μ) and standard deviation (σ) of all control spots were calculated. The Z-score for each compound was calculated as

$$Z\text{-score} = \frac{\text{compound mean} - \mu}{\sigma}$$

Hits were identified using the following three criteria for each compound: spot CV < 100, average spot Z-score > 3, and $|Z\text{-score}| / (Z\text{-score of negative control array}) > 3$. PTP1B slides were compared to slides for a negative control protein. Hits were verified visually using slide images.

Thermal Shift Assay. Recombinant HaloTag protein was diluted in PBS to either 30 μ M or 10 μ M, and then SYPRO Orange (Sigma Aldrich) was diluted 1:1000 into the solution. A 1 μ L volume of various compound concentrations was then placed into each well of a

Low 96-well Clear Multiplate PCR Plate (Bio-Rad) along with 30 μ L of the protein-SYPRO Orange mixture, and the plates were covered with Microseal "B" Film (Bio-Rad). Real-time thermal cycling was then performed using the CFX96 Real-Time System (Bio-Rad). A protein melting curve was then generated between 25 and 100 $^{\circ}$ C using Hex fluorescence readings.

Raw data files were exported from the CFX software, formatted in Microsoft Office Excel, and analyzed using PRISM (GraphPad). Data were trimmed to include the lower limit and upper limit values flanking the transition of interest and were normalized. As described elsewhere,¹² T_m values were calculated as the inflection point of a sigmoidal curve using the Boltzmann equation:

$$y = LL + \frac{UL - LL}{1 + \exp\left(\frac{T_m - x}{a}\right)}$$

where LL is the minimum fluorescence intensity, UL is the maximum fluorescence intensity, and a is the slope of the curve.

p-Nitrophenyl Phosphate Assay. The *p*-nitrophenyl phosphate (pNPP) phosphatase assay was performed in a 96-well plate. Each 101- μ L reaction consisted of 63 μ L of assay buffer (50 mM HEPES, 100 mM NaCl, 2 mM EDTA, 3 mM DTT, 0.1% BSA; pH 7.4), 10 μ L of 1% BSA, 26 μ L of 190 mM *p*-nitrophenyl phosphate (pNPP, Thermo Scientific), 1 μ L of 3 μ M PTP1B, and 1 μ L of compound. Plates were incubated at RT for 10 min. The reactions were then quenched with 100 μ L of 2 M K_2CO_3 , and the absorbance was read at 405 nm using a Wallac Victor 2 1420 plate reader.

■ ASSOCIATED CONTENT

Supporting Information

This material is available free of charge via the Internet.

■ AUTHOR INFORMATION

Corresponding Author

*E-mail: craig.crews@yale.edu.

Notes

The authors declare no competing financial interest.

■ REFERENCES

- (1) Verdine, G. L., and Walensky, L. D. (2007) The challenge of drugging undruggable targets in cancer: lessons learned from targeting BCL-2 family members. *Clin. Cancer Res.* 13, 7264–7270.
- (2) Crews, C. M. (2010) Targeting the undruggable proteome: the small molecules of my dreams. *Chem. Biol.* 17, 551–555.
- (3) Sakamoto, K. M., Kim, K. B., Kumagai, A., Mercurio, F., Crews, C. M., and Deshaies, R. J. (2001) Protacs: chimeric molecules that target proteins to the Skp1-Cullin-F box complex for ubiquitination and degradation. *Proc. Natl. Acad. Sci. U.S.A.* 98, 8554–8559.
- (4) Sakamoto, K. M., Kim, K. B., Verma, R., Ransick, A., Stein, B., Crews, C. M., and Deshaies, R. J. (2003) Development of Protacs to target cancer-promoting proteins for ubiquitination and degradation. *Mol. Cell. Proteomics* 2, 1350–1358.
- (5) Schneekloth, J. S., Jr., Fonseca, F. N., Koldobskiy, M., Mandal, A., Deshaies, R., Sakamoto, K., and Crews, C. M. (2004) Chemical genetic control of protein levels: selective in vivo targeted degradation. *J. Am. Chem. Soc.* 126, 3748–3754.
- (6) Schneekloth, A. R., Puchault, M., Tae, H. S., and Crews, C. M. (2008) Targeted intracellular protein degradation induced by a small molecule: En route to chemical proteomics. *Bioorg. Med. Chem. Lett.* 18, 5904–5908.
- (7) Neklesa, T. K., Tae, H. S., Schneekloth, A. R., Stulberg, M. J., Corson, T. W., Sundberg, T. B., Raina, K., Holley, S. A., and Crews, C. M. (2011) Small-molecule hydrophobic tagging-induced degradation of HaloTag fusion proteins. *Nat. Chem. Biol.* 7, 538–543.
- (8) Tae, H. S., Sundberg, T. B., Neklesa, T. K., Noblin, D. J., Gustafson, J. L., Roth, A. G., Raina, K., and Crews, C. M. (2012) Identification of hydrophobic tags for the degradation of stabilized proteins. *ChemBioChem* 13, 538–541.
- (9) MacBeath, G., Koehler, A. N., and Schreiber, S. L. (1999) Printing Small Molecules as Microarrays and Detecting Protein-Ligand Interactions en Masse. *J. Am. Chem. Soc.* 121, 7967–7968.
- (10) Kuruvilla, F. G., Shamji, A. F., Sternson, S. M., Hergenrother, P. J., and Schreiber, S. L. (2002) Dissecting glucose signalling with diversity-oriented synthesis and small-molecule microarrays. *Nature* 416, 653–657.
- (11) Bradner, J. E., McPherson, O. M., and Koehler, A. N. (2006) A method for the covalent capture and screening of diverse small molecules in a microarray format. *Nat. Protoc.* 1, 2344–2352.
- (12) Niesen, F. H., Berglund, H., and Vedadi, M. (2007) The use of differential scanning fluorimetry to detect ligand interactions that promote protein stability. *Nat. Protoc.* 2, 2212–2221.
- (13) Hergenrother, P. J., Depew, K. M., and Schreiber, S. L. (2000) Small-molecule microarrays: covalent attachment and screening of alcohol-containing small molecules on glass slides. *J. Am. Chem. Soc.* 122, 7849–7850.
- (14) Barnes-Seeman, D., Park, S. B., Koehler, A. N., and Schreiber, S. L. (2003) Expanding the functional group compatibility of small-molecule microarrays: discovery of novel calmodulin ligands. *Angew. Chem., Int. Ed.* 42, 2376–2379.
- (15) Bradner, J. E., McPherson, O. M., Mazitschek, R., Barnes-Seeman, D., Shen, J. P., Dhaliwal, J., Stevenson, K. E., Duffner, J. L., Park, S. B., Neuberg, D. S., Nghiem, P., Schreiber, S. L., and Koehler, A. N. (2006) A robust small-molecule microarray platform for screening cell lysates. *Chem. Biol.* 13, 493–504.
- (16) Marsden, D. M., Nicholson, R. L., Skindersoe, M. E., Galloway, W. R. J. D., Sore, H. F., Givskov, M., Salmond, G. P. C., Ladlow, M., Welch, M., and Spring, D. R. (2010) Discovery of a quorum sensing modulator pharmacophore by 3D small-molecule microarray screening. *Org. Biomol. Chem.* 8, 5313–5323.
- (17) Koehler, A. N., Shamji, A. F., and Schreiber, S. L. (2003) Discovery of an inhibitor of a transcription factor using small molecule microarrays and diversity-oriented synthesis. *J. Am. Chem. Soc.* 125, 8420–8421.
- (18) Shaner, N. C., Steinbach, P. A., and Tsien, R. Y. (2005) A guide to choosing fluorescent proteins. *Nat. Methods* 2, 905–909.
- (19) Los, G. V., Encell, L. P., McDougall, M. G., Hartzell, D. D., Karassina, N., Zimprich, C., Wood, M. G., Learish, R., Ohana, R. F., Urh, M., Simpson, D., Mendez, J., Zimmerman, K., Otto, P., Vidugiris, G., Zhu, J., Darzins, A., Klaubert, D. H., Bulleit, R. F., and Wood, K. V. (2008) HaloTag: a novel protein labeling technology for cell imaging and protein analysis. *ACS Chem. Biol.* 3, 373–382.
- (20) Siekierka, J. J., Hung, S. H., Poe, M., Lin, C. S., and Sigal, N. H. (1989) A cytosolic binding protein for the immunosuppressant FK506 has peptidyl-prolyl isomerase activity but is distinct from cyclophilin. *Nature* 341, 755–757.
- (21) Sehgal, S. N., Baker, H., and Vezina, C. (1975) Rapamycin (AY-22,989), a new antifungal antibiotic. II. Fermentation, isolation and characterization. *J. Antibiot.* 28, 727–732.
- (22) Clackson, T., Yang, W., Rozamus, L. W., Hatada, M., Amara, J. F., Rollins, C. T., Stevenson, L. F., Magari, S. R., Wood, S. A., Courage, N. L., Lu, X., Cerasoli, F., Jr., Gilman, M., and Holt, D. A. (1998) Redesigning an FKBP-ligand interface to generate chemical dimerizers with novel specificity. *Proc. Natl. Acad. Sci. U.S.A.* 95, 10437–10442.
- (23) Bierer, B. E., Mattila, P. S., Standaert, R. F., Herzenberg, L. A., Burakoff, S. J., Crabtree, G., and Schreiber, S. L. (1990) Two distinct signal transduction pathways in T lymphocytes are inhibited by complexes formed between an immunophilin and either FK506 or rapamycin. *Proc. Natl. Acad. Sci. U.S.A.* 87, 9231–9235.
- (24) Bandyopadhyay, D., Kusari, A., Kenner, K. A., Liu, F., Chernoff, J., Gustafson, T. A., and Kusari, J. (1997) Protein-tyrosine phosphatase 1B complexes with the insulin receptor in vivo and is tyrosine-phosphorylated in the presence of insulin. *J. Biol. Chem.* 272, 1639–1645.
- (25) Zabolotny, J. M., Bence-Hanulec, K. K., Stricker-Krongrad, A., Haj, F., Wang, Y., Minokoshi, Y., Kim, Y. B., Elmquist, J. K., Tartaglia, L. A., Kahn, B. B., and Neel, B. G. (2002) PTP1B regulates leptin signal transduction in vivo. *Dev. Cell* 2, 489–495.

- (26) Elchebly, M., Payette, P., Michaliszyn, E., Cromlish, W., Collins, S., Loy, A. L., Normandin, D., Cheng, A., Himms-Hagen, J., Chan, C. C., Ramachandran, C., Gresser, M. J., Tremblay, M. L., and Kennedy, B. P. (1999) Increased insulin sensitivity and obesity resistance in mice lacking the protein tyrosine phosphatase-1B gene. *Science* 283, 1544–1548.
- (27) Zinker, B. A., Rondinone, C. M., Trevillyan, J. M., Gum, R. J., Clampit, J. E., Waring, J. F., Xie, N., Wilcox, D., Jacobson, P., Frost, L., Kroeger, P. E., Reilly, R. M., Koterski, S., Oppenorth, T. J., Ulrich, R. G., Crosby, S., Butler, M., Murray, S. F., McKay, R. A., Bhanot, S., Monia, B. P., and Jirousek, M. R. (2002) PTP1B antisense oligonucleotide lowers PTP1B protein, normalizes blood glucose, and improves insulin sensitivity in diabetic mice. *Proc. Natl. Acad. Sci. U.S.A.* 99, 11357–11362.
- (28) You-Ten, K. E., Muise, E. S., Itie, A., Michaliszyn, E., Wagner, J., Jothy, S., Lapp, W. S., and Tremblay, M. L. (1997) Impaired bone marrow microenvironment and immune function in T cell protein tyrosine phosphatase-deficient mice. *J. Exp. Med.* 186, 683–693.
- (29) Comeau, A. B., Critton, D. A., Page, R., and Seto, C. T. (2010) A focused library of protein tyrosine phosphatase inhibitors. *J. Med. Chem.* 53, 6768–6772.
- (30) Brandão, T. A., Hengge, A. C., and Johnson, S. J. (2010) Insights into the reaction of protein-tyrosine phosphatase 1B: crystal structures for transition state analogs of both catalytic steps. *J. Biol. Chem.* 285, 15874–15883.
- (31) Blair, A. J., Pantony, D. A., and Minkoff, G. J. (1958) The chemistry of some 8-hydroxyquinoline complexes of vanadium. *J. Inorg. Nucl. Chem.* 5, 316–331.